The Effect of Carbon on the Microstructure and Properties of C-Mn All-Weld Metal Deposits

Carbon promotes acicular ferrite, at the expense of grain boundary polygonal ferrite, and causes grain refinement of the reheated regions

BY G. M. EVANS

SYNOPSIS. The effect of 0.05 to 0.15% carbon on the microstructure and properties of shielded metal arc welds containing 0.6 to 1.8% Mn has been investigated. It was found that carbon promoted acicular ferrite, at the expense of grain boundary polygonal ferrite, and caused grain refinement of the reheated regions. The hardness of the deposits increased, and the tensile properties were defined by equations of the form:

$$\sigma = a + b\,(C) + c\,(Mn) + d\,(C \cdot Mn).$$

With regard to impact properties, it was found that carbon tilted the Charpy-V curves and substantially reduced the degree of scattering. Optimum toughness was achieved at a manganese level of 1.4% when the carbon content was in the intermediate range, *i.e.,* 0.07 to 0.09%.

Introduction

Previous work (Ref. 1), conducted as part of a joint program within Sub-Commission IIA of the International Institute of Welding, established, for low carbon deposits, that manganese increasingly refines weld metal microstructures and gives rise to optimum impact properties at a concentration of about 1.5%.

The present work is a continuation of the program. Its main aim is to ascertain whether the optimum with regard to manganese is displaced, depending on the carbon level of the deposit.

Paper selected as an alternate for the 64th AWS Annual Convention, Philadelphia, Pennsylvania, April 24-29, 1983.

G. M. EVANS is with Welding Industries Oerlikon Buehrle Ltd., Zurich, Switzerland.

Experimental Procedure

Electrodes

Low hydrogen, iron powder type electrodes — coded A, B, C and D — were prepared as in previous work (Ref. 1). The manganese content of the coverings was varied to yield deposited metals containing 0.6, 1.0, 1.4 and 1.8% Mn, respectively.

At each of these manganese levels different amounts of graphite were added to the coatings to produce four nominal levels of carbon in the deposited metals — namely, 0.045, 0.065, 0.095 and 0.145% C. The core wire diameter of the 16 batches of experimental electrodes thus prepared was 4 mm (0.16 in.), and the coating factor (D/d) was 1.68.

Weld Preparation

The joint geometry was that specified in ISO 2560. Welding was done in the flat position, and three weld beads per layer were deposited (Ref. 1). The total number of runs required to fill the individual joints was 27. Direct current (electrode positive) was employed, the amperage being 170 A, the voltage 21 V, and the heat-input was nominally 1 kJ/mm (25 kJ/in.). The interpass temperature was standardized at 200°C (392°F).

Mechanical Testing

Two subsize weld metal tensile specimens were machined and tested for each of the different deposits. Also, approximately 35 Charpy-V notch specimens were struck to obtain a full transition curve. The impact specimens were in the as-welded condition. On the other hand, the tensile specimens underwent hydrogen removal treatment at 250°C (482°F) for 14 hours (h).

Results

Chemical Composition

The chemical analyses of the weld metal deposits are given in Table 1. The compositions were essentially on target, the nominal values for carbon being 0.045, 0.065, 0.095 and 0.145% at each of the four manganese levels previously (Ref. 1) designated as A, B, C and D. The silicon contents were relatively well balanced, the increase with increasing carbon being slight. Of note is the fact that both sulfur and phosphorus were low throughout.

Metallographic Examination

General. Transverse sections were prepared, and detailed examination was carried out on the top weld beads and on the adjacent super critically heat-affected zones as described previously (Ref. 1).

To illustrate the changes due to carbon, as observed in the light microscope, typical micrographs for the extremes are shown in Figs. 1–4 for the 1.4% Mn level.

As-Deposited Weld Metal. The top weld bead of each of the test weldments was examined at the Welding Institute, U.K., and the microstructural components were quantified according to the scheme proposed by Abson and Dolby (Ref. 2) and by Pargeter (Ref. 3).

Point counting was carried out at ×500, and the constituents were identified as follows:

- Grain boundary ferrite.
- Polygonal ferrite.
- Ferrite with aligned M-A-C.
- Acicular ferrite.

Table 1—Weld Metal Chemical Compositions and Tensile Properties

Average carbon content, %	Electrode designation	Composition, %					Tensile properties(a)			
		C	Mn	Si	5	P	σ_E, N/mm^{2}(b)	σ_R, N/mm^{2}(b)	El., %	R.A., %
0.045	A	0.045	0.65	0.30	0.006	0.008	406	462	35.4	78.8
	B	0.044	0.98	0.32	0.006	0.008	432	481	35.8	78.8
	C	0.044	1.32	0.32	0.006	0.007	451	512	32.0	78.8
	D	0.045	1.72	0.30	0.006	0.008	488	549	29.6	76.0
0.065	A	0.059	0.60	0.33	0.007	0.008	407	483	31.2	80.6
	B	0.063	1.00	0.35	0.006	0.008	451	516	32.4	80.6
	C	0.066	1.35	0.37	0.005	0.007	469	545	29.2	78.8
	D	0.070	1.77	0.33	0.006	0.008	511	588	28.4	77.9
0.095	A	0.099	0.65	0.35	0.008	0.009	433	512	31.8	78.8
	8	0.098	1.05	0.32	0.007	0.009	477	546	30.0	78.8
	C	0.096	1.29	0.30	0.007	0.009	506	576	30.8	77.9
	D	0.093	1.65	0.33	0.007	0.007	535	602	27.8	74.0
0.145	A	0.147	0.63	0.40	0.008	0.007	480	569	32.8	76.0
	B	0.152	1.00	0.41	0.007	0.007	517	605	27.4	75.0
	C	0.148	1.40	0.38	0.007	0.007	536	636	27.4	75.7
	D	0.141	1.76	0.36	0.006	0.007	606	691	25.6	71.9

(a) σ_E = yield stress; σ_R = ultimate tensile stress; El. = elongation; R.A. = reduction in area.
(b) psi = 145.0377 × N/mm^2.

- Ferrite-carbide aggregate.
- Carbide.

The quantitative data obtained are plotted in Fig. 5; they show that the amount of grain boundary ferrite and polygonal ferrite decreased as the carbon content was increased. In the main, the change was compensated for by an increase in the amount of acicular ferrite rather than an increase in the proportion of the side plate structures, *i.e.*, ferrite with M-A-C. The ferrite-carbide aggregate also increased but only at the lowest levels of manganese.

A visual impression of the microstructural change in the top bead is obtained from Fig. 1. Here it is seen that the measured reduction in polygonal ferrite is reflected in thinner ferrite veins. Of further note is the fact that the columnar grain width also decreased. This latter phenomenon is quantified in Fig. 6, the main variation occurring over the lower end of the investigated carbon range. An additional point is that the average grain width was slightly reduced throughout by the addition of manganese.

Examination of the acicular ferrite in Fig. 2 shows changes in the aspect ratio of the ferrite laths; the structure at the higher carbon level is more classically Widmanstätten in nature. A further observed difference is in the size of the microphase regions occurring between the laths. Subsequent examination in the scanning electron microscope (SEM) confirmed that amounts of these martensite / austenite (M / A) phases increased substantially as the carbon content was increased.

Reheated Weld Metal. Studies of the coarse grained regions also revealed differences in microstructure as exemplified in Fig. 3. With increasing carbon, the width of the ferrite envelopes delineating

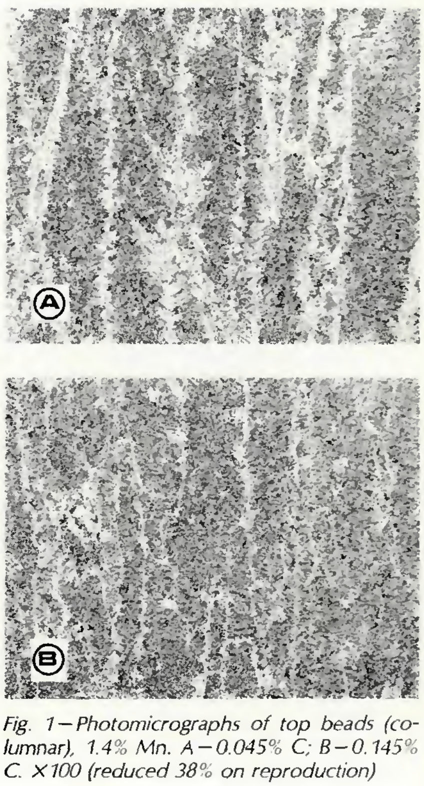

Fig. 1—Photomicrographs of top beads (columnar), 1.4% Mn. A—0.045% C; B—0.145% C. ×100 (reduced 38% on reproduction)

Fig. 2—Photomicrographs of acicular ferrite in columnar regions, 1.4% Mn. A—0.045% C; B—0.145% C. ×100 (reduced 38% on reproduction)

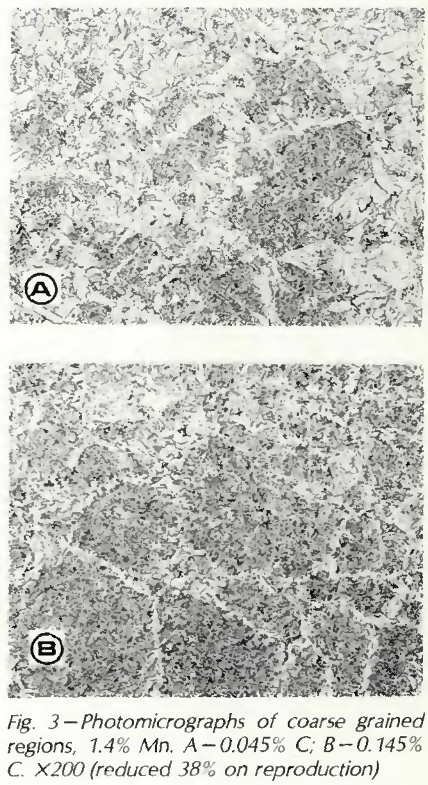

Fig. 3—Photomicrographs of coarse grained regions, 1.4% Mn. A—0.045% C; B—0.145% C. ×200 (reduced 38% on reproduction)

the prior austenite grain boundaries decreased and thus enhanced the etching response. The grain interiors transformed to a fine acicular structure, and the changes were essentially a reflection of those occurring in the as-deposited weld metal.

Comparison of the two photomicrographs in Fig. 4 shows that grain refinement also occurred in the fine grained reheated regions. The results of linear intercepts made at ×630 are plotted in Fig. 7. The effects of carbon and manganese were found to be approximately equivalent over the experimental ranges investigated. The microstructure became more duplex with increasing carbon as shown in Fig. 4, and the second phases tended to separate, to an increasingly greater extent, along the primary segregation bands. The form and structure of the second phase particles were revealed by deep etching in a mixture of bromine and methanol, followed by examination in the SEM at ×5000 magnification. The phases were identified, by the British Steel Corporation, as:

- Cementite films.

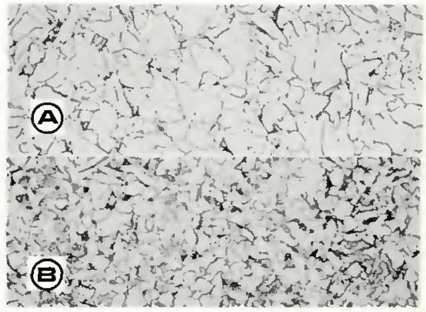

Fig. 4 — Photomicrographs of fine grained regions, 1.4% Mn. A — 0.045% C; B — 0.145% C. X630 (reduced 38% on reproduction)

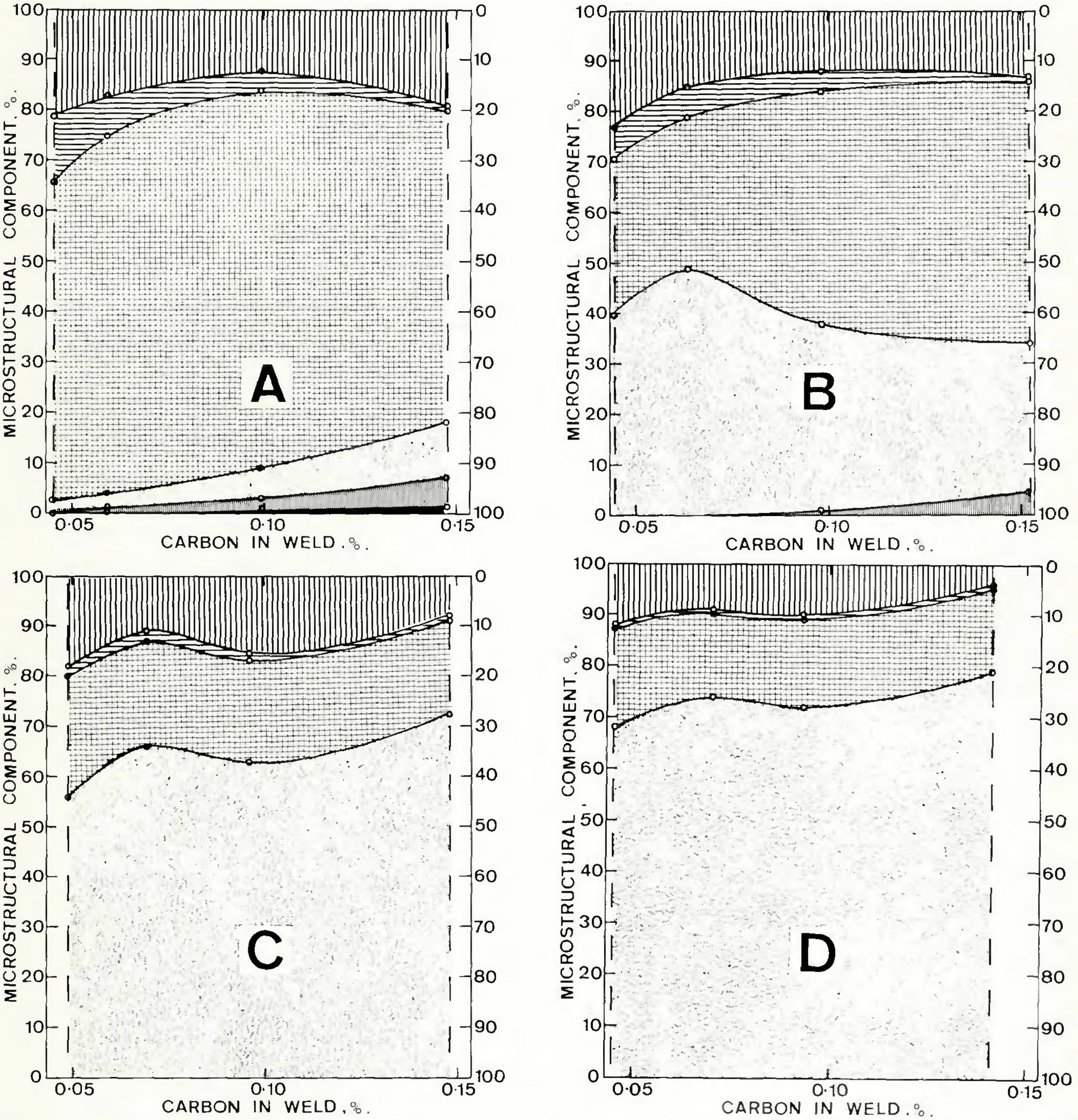

Fig. 5 — Effect of carbon on the microstructure of weld metals obtained using electrodes A, B, C, and D with Mn in coverings varied to yield deposit metals containing Mn as follows: electrode A — 0.6% Mn, electrode B — 1.0% Mn, electrode C — 1.4% Mn and electrode D — 1.8% Mn

- Martensite / austenite (M / A).
- Bainite / Fine pearlite (B / P).

The volume fractions were found to increase with increasing carbon content as shown in Figs. 8 and 9 for the 0.6 and 1.4% Mn levels, respectively.

Hardness Testing

Average hardness values, obtained for the last weld bead to be deposited in each case, are plotted in Fig. 10. The trends are essentially linear, the increase over the range for manganese being 50 DPN (*i.e.*, VHN) compared to approximately 30 DPN (*i.e.*, VHN) for the experimental range of carbon contents.

Hardness traverses along the center line of deposits welded with electrode C, at the two extremes of carbon, are plotted in Fig. 11; the difference of 30 DPN (*i.e.*, VHN), as encountered for the top beads, is reflected throughout most of the weldments.

Mechanical Properties

Tensile Results. The tensile test results are presented in Table 1. The yield strengths and the ultimate tensile

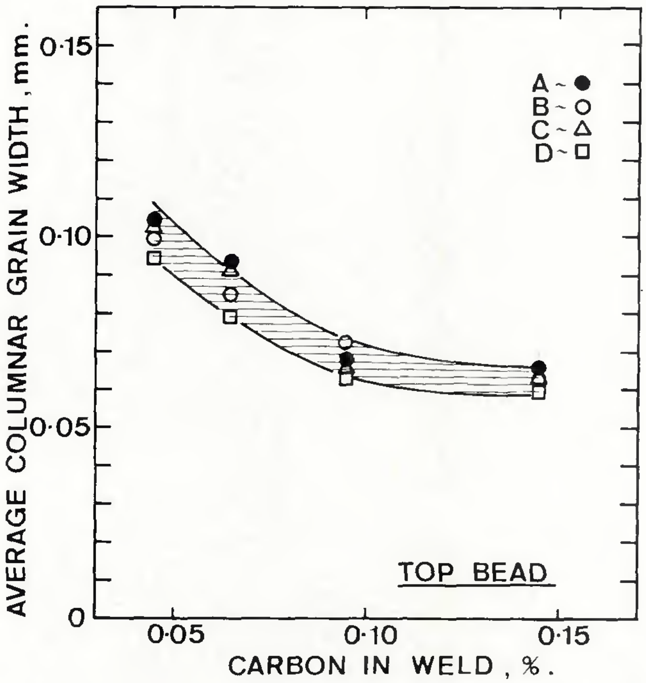

Fig. 6 — Effect of carbon content on the average columnar grain width at different manganese levels as follows: A — 0.6%; B — 1.0%, C — 1.4% and D — 1.8%

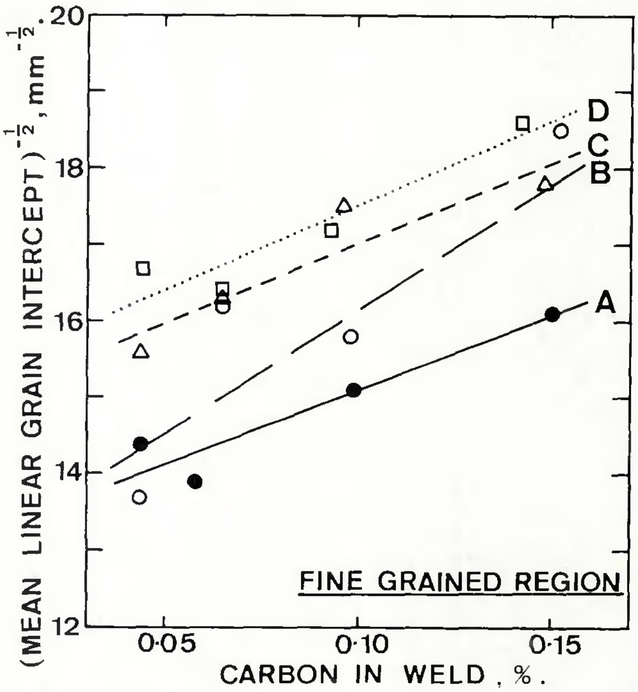

Fig. 7 — Effect of carbon on the grain intercept in the fine grained region at different manganese levels as follows: A — 0.6%, B — 1.0%, C — 1.4% and D — 1.8%

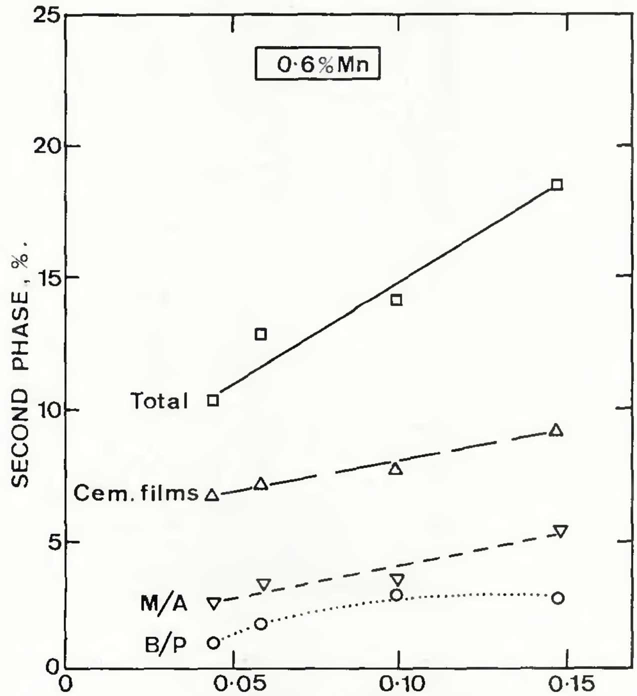

Fig. 8 — Effect of carbon content on percentage microphases in fine grained regions, 0.6% Mn

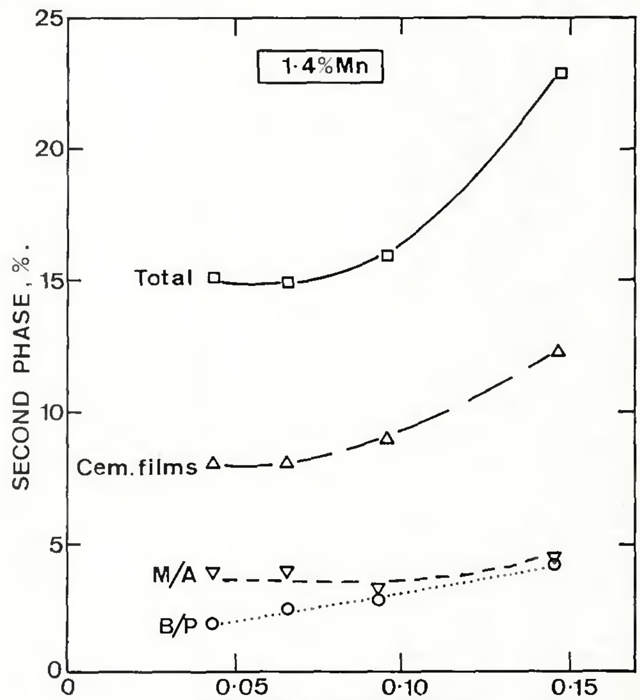

Fig. 9 — Effect of carbon content on percentage microphases in fine grained regions, 1.4% Mn (cementite films, martensite/austenite, bainite/pearlite)

strengths are plotted against carbon content in Figs. 12 and 13, respectively. On assuming the tensile properties to be linearly related to both carbon and manganese, the following regressions were obtained:

1. For yield strength (in N/mm^2):

$$\sigma_E = 335 + 439\ C + 60\ Mn + 361\ C \cdot Mn \quad (1)$$

2. For ultimate tensile strength (in N/mm^2):

$$\sigma_R = 379 + 754\ C + 63\ Mn + 337\ C \cdot Mn \quad (2)$$

Impact Results. Charpy-V impact curves, obtained from the average of the scatter bands, are plotted in Fig. 14. It is seen that the upper shelf was depressed by the addition of carbon, whereas the lower shelf tended to be raised.

On reconsidering the absorbed energy as a function of manganese (Fig. 15), the optimum composition for the transition range was found to occur at about 1.4% Mn, independently of the carbon level of the deposits.

The relative effects of carbon and manganese on lateral shift are depicted in Fig. 16. Here the Charpy-V temperatures corresponding to an arbitrary level of 100 J are plotted against composition. At the low manganese level (A), carbon was found to be marginally beneficial, whereas at the high level (D) carbon was deleterious. For the intermediate manganese content (C), optimum toughness was achieved at an intermediate carbon content of 0.09%. Comparison of the two graphs in Fig. 16 shows, for the specific ranges, that manganese had a far greater influence on lateral shift than carbon.

An additional feature to the tilting of the average Charpy-V curves was the observed fact that the degree of scattering decreased as the carbon content increased. The phenomenon is illustrated in Fig. 17 for the two extremes of carbon at the 1.4% Mn level. The situation for the low carbon level is seen to be undesirable, the transition being extremely steep and such that full bi-modal fracture occurred at −40°C (−40°F).

Discussion

It is generally accepted (Refs. 4–6) that the addition of carbon to low strength ferritic weld metal causes the yield and tensile strengths to increase and ductility to decrease. Furthermore, the hardness increases and, at a constant grain size, the yield-to-tensile strength ratio decreases. The role of different alloying elements is known to be complex; carbon in isolation, for example, behaves differently

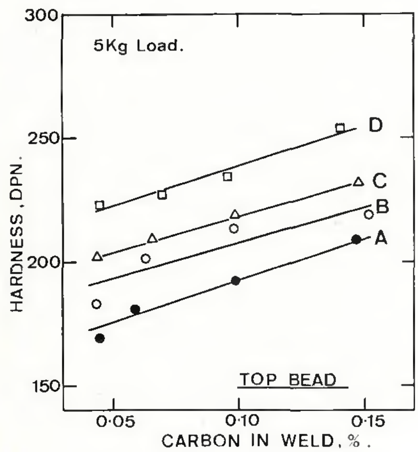

Fig. 10 — Effect of carbon on hardness of as-deposited weld metal at different manganese levels as follows: A — 0.6%, B — 1.0%, C — 1.4% and D — 1.8%

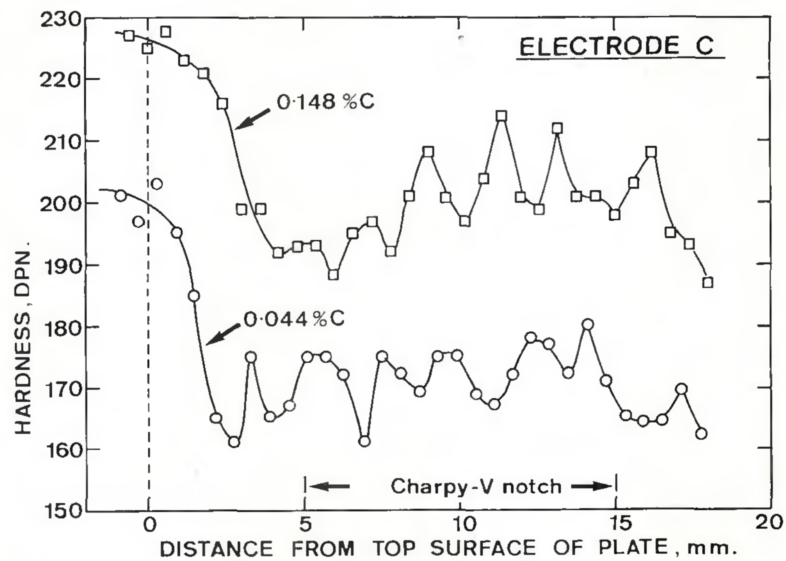

Fig. 11. — Effect of carbon on yield stress at different manganese levels as follows: A — 0.6%, B — 1.0%, C — 1.4% and D — 1.8%

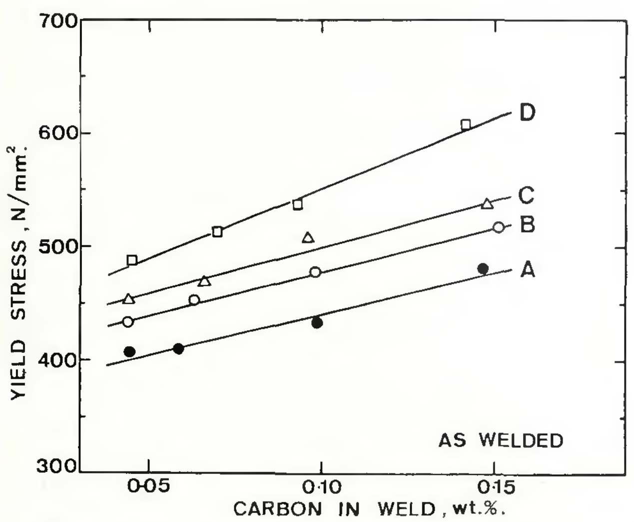

Fig. 12 — Effect of carbon on yield stress at different manganese levels as follows: A — 0.6%, B — 1.0%, C — 1.4% and D — 1.8%

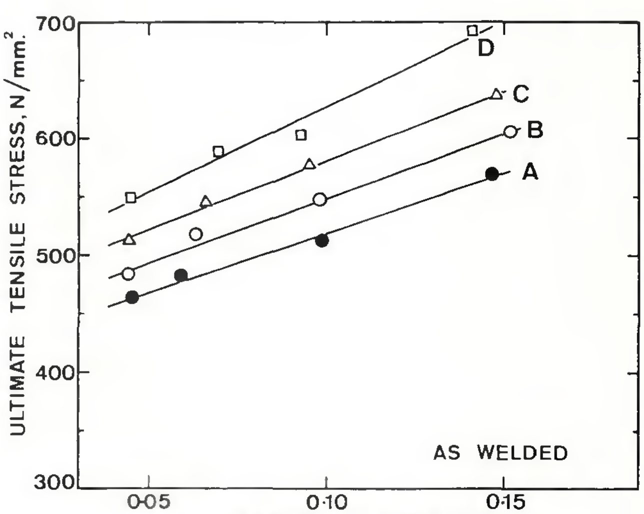

Fig. 13 — Effect of carbon on ultimate tensile strength at different manganese levels as follows: A — 0.6%, B — 1.0%, C — 1.4% and D — 1.8%

than when in the presence of manganese, silicon and oxygen (Ref. 7).

The present metallographic studies have shown that the microstructure of as-deposited weld metal is modified by the addition of carbon. On a macroscale, the main observation was that the prior austenite grain width decreased, due possibly to a change in the solidification sub-structure. Carbon was more effective in this respect than manganese, and it is presumed that the relative effects on dendrite spacing are different.

On a microscale, carbon was found to increase the amount of acicular ferrite at the expense of the proeutectoid ferrite occurring at the boundaries of the columnar grains. For an increment of 0.1% C, however, the overall change in microstructure was far less than that encountered when varying the manganese content over the range from 0.6 to 1.8%. On the other hand, increasing carbon did lead to the precipitation of increasing amounts of carbide within the acicular ferrite.

The microstructure of the reheated zones was also modified by the addition of carbon. In the case of the coarse grained regions, the ferrite envelopes tended to be eliminated, and in the fine grained regions the grain size decreased appreciably. The degree of grain refinement induced by the increase in carbon was essentially the same as that encountered for the experimental range of manganese contents. As expected, the amount of second phase carbides in the fine grained regions increased as the carbon level was raised.

The tensile properties achieved in the present instance varied linearly with respect to both carbon and manganese, the regression equations being in the form:

$$\sigma = a + b\,(C) + c\,(Mn) + d\,(C \cdot Mn).$$

Interaction occurred as indicated by the lines in Figs. 12 and 13 which are not parallel. This is as expected, since it is known, for wrought materials, that both elements have an effect on solid solution hardening, grain size and the percentage amount of pearlite (Ref. 8).

The present data serve to confirm the statement made by Heuschkel (Ref. 9) that, for all practical purposes, there is little error in assuming 0.04 to 0.14%

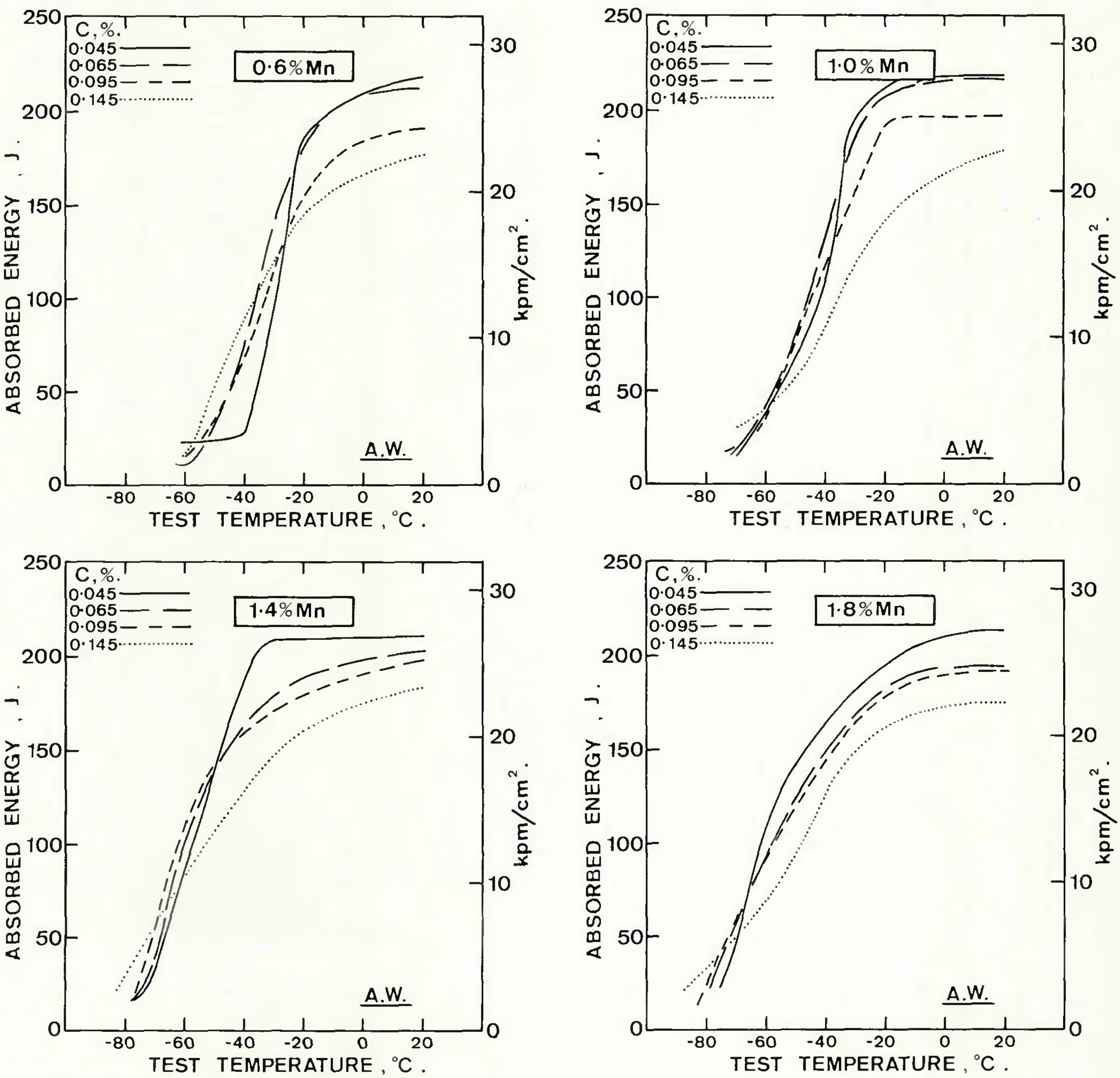

Fig. 14—Charpy V-notch test results, as-welded

carbon increases yield strength in a linear manner. Straight line relationships have been obtained previously for manganese, the specific constants being dependent on process variables, such as interpass temperature (Ref. 10) and heat-input (Ref. 11).

The addition of carbon to the weld deposits modified the shape of the Charpy-V curves by lowering the upper shelf energy values and making the transition between the ductile and the brittle mode of fracture more gradual. Thus, with increasing hardenability, the critical inclusion distance decreased and the second phases increasingly served as sites for micro-void coalescence.

Allen, *et al.* (Ref. 12), have suggested that carbide films contribute to the change in slope of the transition curves. Also, den Ouden, *et al.* (Ref. 7), proposed that flattening occurs to a greater extent when carbon is present together with a certain amount of oxygen. At the lower end of the transition range, carbon was beneficial to an extent that depended on manganese; also, the detrimental influence of carbides on cleavage (Ref. 12) was evidently compensated for by the reduction in grain size. The overall situation was such that the optimum with regard to manganese remained at approximately 1.4%, independent of the carbon content—Fig. 15. This finding is contrary to that expected and indicates that dilution with a high carbon base material cannot be compensated for by lowering the manganese level.

Moll and Stout (Ref. 13) and den Ouden, *et al.* (Ref. 7), have shown that commercial weldments have comparable if not better transition characteristics than deposits synthesized from pure raw materials. In addition, Sagan and Campbell (Ref. 4) refer to an instance where a low carbon content is by no means desirable. In that case, an extra low carbon E7018 electrode, produced with an ingot-iron core wire, gave a room temperature upper shelf value in excess of 360 J but was inferior to a commercial product at −20°C (−4°F). The requirement, therefore, is for an intermediate carbon level so that the upper shelf is not depressed too much while still tilting the curve sufficiently and limiting the scatter band—Fig. 17.

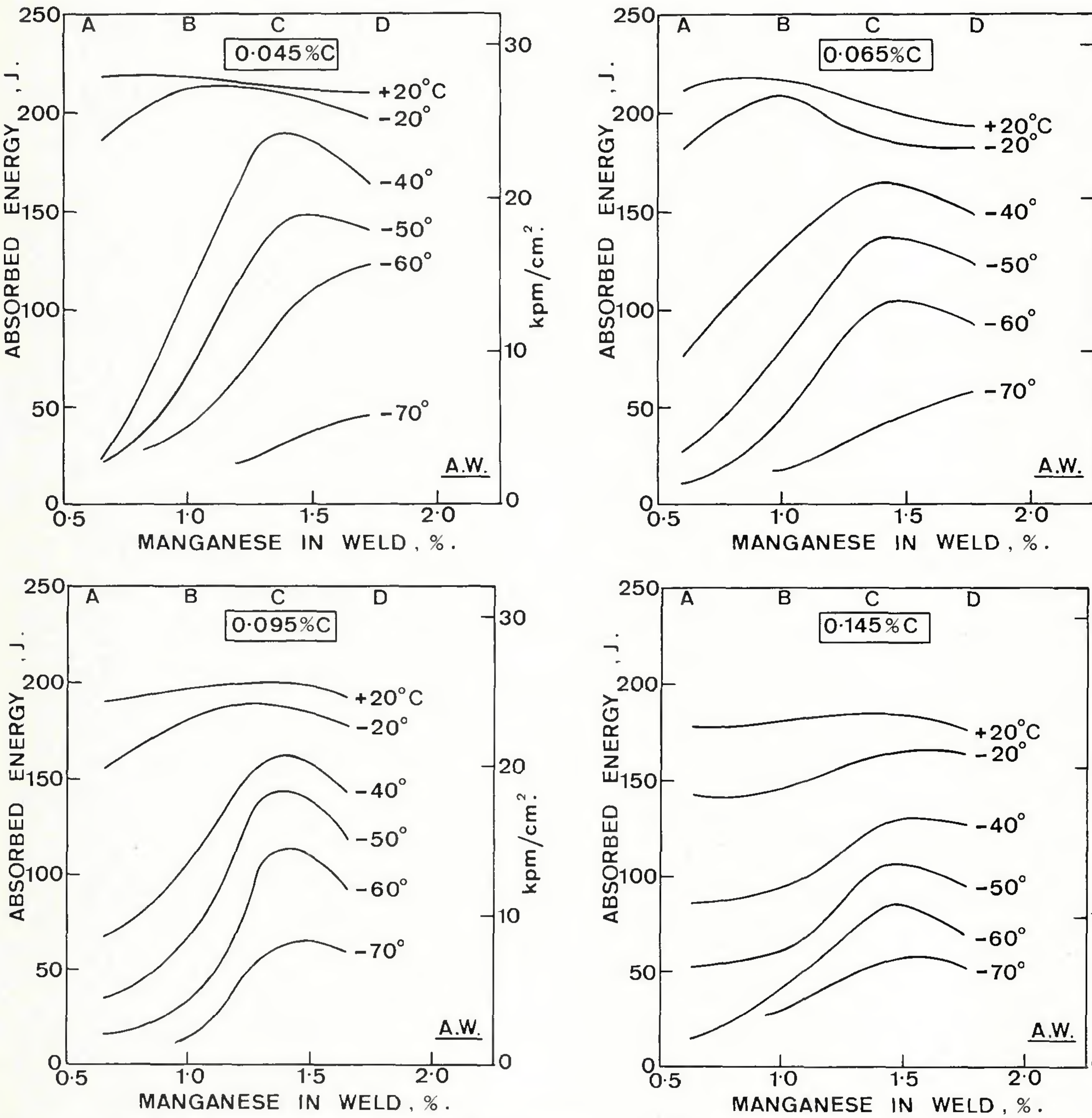

Fig. 15—Effect of manganese on energy absorbed at different temperatures for different carbon levels

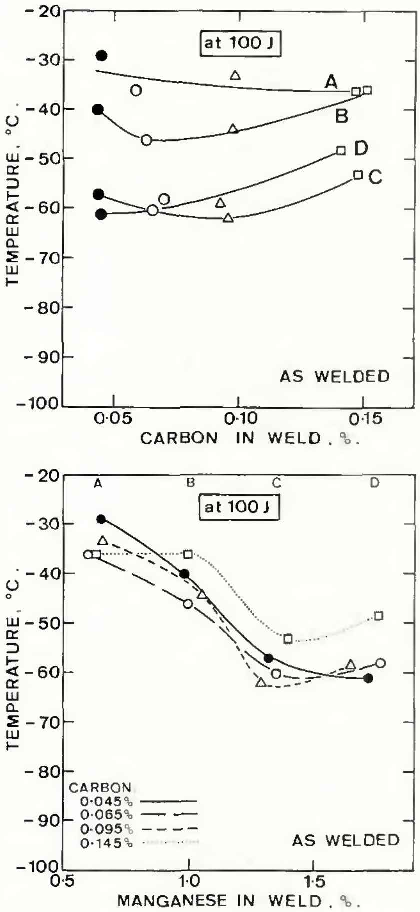

Fig. 16—Effects of carbon and manganese on test temperatures corresponding to 100 J

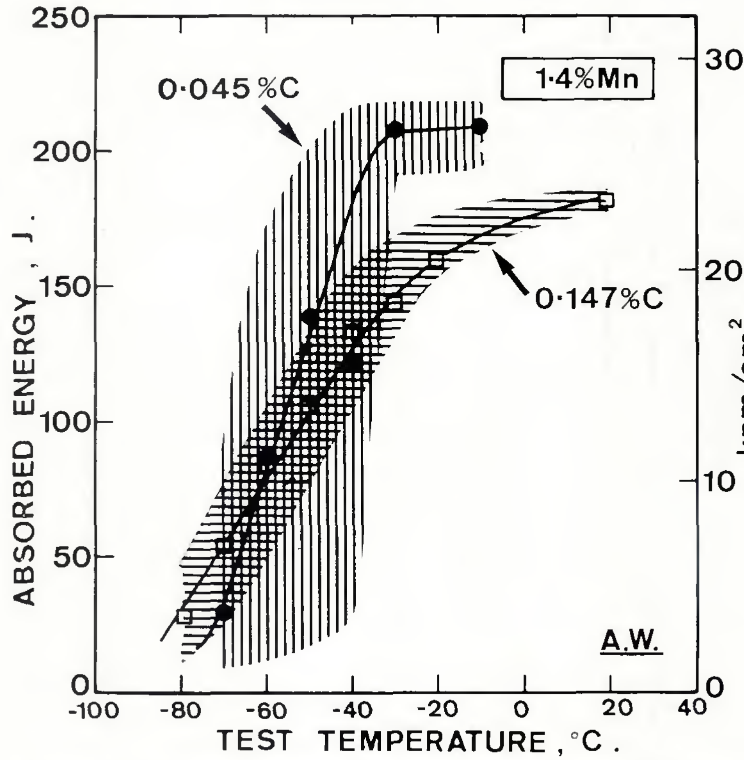

Fig. 17—Charpy V-notch impact curves showing scatter bands for low and high carbon levels at 1.4% Mn

For E7018 electrodes, which have been permitted to yield up to 1.6% Mn since the introduction of AWS A5.1-78 (Ref. 14), the most suitable range suggested by the results of the present work is between approximately 0.07 and 0.09% carbon.

Conclusion

For ISO 2560 type deposited metal, welded with basic iron powder electrodes of a specific slag base type, the following occurred on increasing the carbon content:

1. The average width of the prior austenite grains decreased.
2. The amount of acicular ferrite increased at the expense of the proeutectoid ferrite.
3. The aspect ratio of the acicular ferrite changed, increasing the amount of carbide formed between the laths.
4. Grain refinement occurred in the high temperature reheated regions.
5. Grain refinement occurred in the low temperature reheated regions.
6. Increasing amounts of second phases were precipitated in the fine grained regions.
7. The hardness increased.
8. The yield and tensile strengths increased linearly, both parameters being defined by equations of the form:

$$\sigma = a + b(C) + c(Mn) + d(C \cdot Mn).$$

9. The Charpy-V curves were tilted, the upper shelf being depressed whereas the lower shelf was raised.
10. The degree of scattering in the Charpy V-notch test was reduced.
11. Notch toughness improved at low manganese levels and deteriorated at high manganese levels.
12. At an intermediate manganese content (1.4%), the toughness initially improved and then deteriorated, an optimum occurring in the range 0.07 to 0.09% C.
13. At any specific carbon content, optimum toughness was encountered at 1.4% Mn.

Acknowledgments

The author wishes to express his thanks to Dr. D. J. Abson and Mr. R. J. Pargeter of the Welding Institute and to Dr. R. C. Cochrane of the British Steel Corporation for conducting most of the metallographic part of the present work under contract.

References

1. Evans, G. M. 1980. The effect of manganese on the microstructure and properties of all-weld-metal deposits. *Welding Journal* 59(3):67-s to 75-s.
2. Abson, D. J., and Dolby, R. E. *A scheme for the quantitative description of ferritic weld metal microstructures.* IIW document IX-J-29-80.
3. Pargeter, R. J. *Quantification of ferritic weld metal microstructures—results of an international exercise.* IIW document IX-J-37-80.
4. Sagen, S. S., and Campbell, H. C. 1960 (April). *Factors which affect low-alloy weld metal notch toughness.* Welding Research Council bulletin no. 59.
5. Masubuchi, K., Monroe, R. E., and Martin, D. C. 1966 (January). *Interpretive report on weld-metal toughness.* Welding Research Council bulletin no. 111.
6. Dorschu, K. E. 1977 (October). *Factors affecting weld metal properties in carbon and low alloy pressure vessel steels.* Welding Research Council bulletin no. 231.
7. den Ouden, G., Verhagen, J. G., and Tichelaar, G. W. 1975. Influence of chemical composition on mild steel weld metal notch toughness. *Welding Journal* 54(3):87-s to 94-s.
8. Pickering, F. B. 1978. *Physical metallurgy and the design of steels.* Applied Science Publishers Ltd.
9. Heuschkel, J. 1973. 1972 Adams Lecture: weld metal property selection and control. *Welding Journal* 52(1):1-2 to 25-s.
10. Evans, G. M. 1982. Effect of interpass temperature on the microstructure and properties of C-Mn all-weld-metal deposits. *Welding Review* 1(1):14-20.
11. Evans, G. M. 1982. Effect of heat-input on the microstructure and properties of C-Mn all-weld-metal deposits. *Welding Journal* 61(4):125-s to 132-s.
12. Allen, N. P., Rees, W. P., Hopkins, B. E., and Tipler, H. R. 1953. Tensile and impact properties of high-purity iron-carbon-manganese alloys of low carbon content. *J. Iron and Steel Inst.* 174:108.
13. Moll, R. A., and Stout, R. D. 1967. Composition effects in iron-base weld metal. *Welding Journal* 46(12):551-s to 561-s.
14. American Welding Society. 1978. *Specification for carbon steel covered arc welding electrodes.* AWS A5.1-78.